Science and Technology Indonesia
e-ISSN:2580-4391 *p*-ISSN:2580-4405
Vol. 8, No. 3, July 2023

Research Paper

Synthesis, Characterization of Chitosan-ZnO/CuO Nanoparticles Film, and its Effect as an Antibacterial Agent of *Escherichia coli*

Ahmad Fatoni[1*], Agnes Rendowati[1], Lasmaryna Sirumapea[1], Lidya Miranti[1], Siti Masitoh[2], Nurlisa Hidayati[3]

[1]*Bhakti Pertiwi High School of Pharmacy Science, Palembang, South Sumatera, 30128, Indonesia*
[2]*Undergraduate School of Bhakti Pertiwi High School of Pharmacy Science, Palembang, South Sumatera, 30128, Indonesia*
[3]*Department of Chemistry, Faculty of Mathematic and Natural Sciences, Sriwijaya University, Indralaya, Ogan Ilir, South Sumatera, 30862, Indonesia*
***Corresponding author**: ahfatoni@yahoo.com

Abstract
The film of chitosan- ZnO/CuO nanoparticles was synthesized. This study were the synthesis and characterization of the chitosan-ZnO/CuO nanoparticles film and its effect as an antibacterial of *Escherichia coli*. The ZnO, CuO, and ZnO/CuO were biosynthesized by biological method and for the synthesis of the chitosan-ZnO/CuO nanoparticles film, the casting method was adopted. The product was analyzed by FTIR spectroscopy, X-ray diffraction (XRD), and Scanning Electron Microscope (SEM), respectively. The product of chitosan-ZnO/CuO nanoparticles film as paper disk and agar disk diffusion method was selected to study an antibacterial agent of this product. The Zn-O or Cu-O group was observed at a peak between 468-675 cm^{-1} for ZnO and 503 and 619 cm^{-1} for CuO nanoparticles, respectively. ZnO, CuO, and ZnO/CuO nanoparticles are in the crystalline form and it has a crystallite size of 13.21, 13.21, and 11.49 nm respectively. After interacting with chitosan, the metal nanoparticles such as ZnO, CuO, and ZnO/CuO nanoparticles can change the crystalline form of chitosan to be amorphous form. The addition of ZnO, CuO, and ZnO/CuO nanoparticles in the chitosan will change the surface morphology of chitosan. Chitosan-ZnO/CuO nanoparticles film can inhibit the growth of *Escherichia coli* bacteria.

Keywords
Chitosan-ZnO/CuO Nanoparticles Film, Characterization, *Escherichia coli*

Received: 31 October 2022, Accepted: 30 May 2023
https://doi.org/10.26554/sti.2023.8.3.373-381

1. INTRODUCTION

The method for synthesis of ZnO/CuO can be done by chemical (Das and Srivastava, 2017; Goyal et al., 2021; Shinde et al., 2022; Saravanakkumar et al., 2018; Alzahrani, 2018; Jayaramudu et al., 2019) and not chemical method such as a biological method (Fouda et al., 2020; Adeyemi et al., 2022; Cao et al., 2021). The major synthesis of metal nanoparticles is divided into three methods: physical, chemical, and biological methods (Naveed Ul Haq et al., 2017). Metal nanoparticles such as CuO and ZnO nanoparticles can be synthesized by chemical (Asamoah et al., 2020), biological (Mohamed, 2020; Jan et al., 2021), and physical methods (Gondal et al., 2013; Al-Dahash et al., 2018). Bloch et al. (2021) reported that the advantages of the synthesis of metal nanoparticles by the physical, chemical, and biological methods are that toxic chemicals are not used, high product, and easy, respectively. But the disadvantages are the expensive instrumentation, toxic chemicals, and difficulty to control the size of metal nanoparticles in the synthesis of metal nanoparticles by physical, chemical, and biological methods, respectively. On other hand, the researchers have chosen a biological method than a physical and chemical method. A cheap method is a base in the synthesis of metal nanoparticles by biological method (Pantidos and Horsfall, 2014). The effect of pH, the concentration of reactant, reaction time, and temperature are a challenge in this method (Zhang et al., 2020).

The researchers made a combination between metal oxide nanoparticles 1 and metal oxide nanoparticles 2 such as ZnO and CuO nanoparticles. This combination aims to increase sensitive biosensors (Solanki et al., 2011; Goyal et al., 2021), antibacterial (Saravanakkumar et al., 2018), photocatalysts (Fouda et al., 2020), and cytotoxicity properties (Cao et al., 2021).

Chitosan can be formed in film form. The flexibility of chitosan film is an advantage of chitosan film (Estevam et al., 2012) but in the film form, chitosan can't inhibit the growth of bacterial (Foster and Butt, 2011).To increase the character of chitosan film, the researchers are using inorganic metal oxide (ZnO nanoparticles) to form chitosan-ZnO nanocom-

posite film as an antibacterial agent (Rahman et al., 2018) and ZnO/CuO nanoparticles to form chitosan-ZnO/CuO nanoparticles film for photodegradation and solar irradiation (Alzahrani, 2018). In this study, the first, the ZnO, CuO, and ZnO/CuO nanoparticles were biosynthesized by biological method and it is different from previous literature (Alzahrani, 2018; Jayaramudu et al., 2019). The second, the ZnO, CuO, and ZnO/CuO nanoparticles are used as modifier agents for chitosan respectively and all of the products are in the film form. All films are prepared by casting method. The characterization of this film with Fourier Transforms Infrared Spectroscopy (FTIR), Scanning Electron Microscopy (SEM), and X-ray Diffraction (XRD). Application of all the films is as antibacterial of *Escherichia coli* with the agar diffusion method.

2. EXPERIMENTAL SECTION

2.1 Materials and Instruments

Chitosan with DD 87% (CV. Ocean Fresh Bandung, West Java, Indonesia). Zinc acetate pentahydrate (Merck), copper sulphate pentahydrate (Merck), sodium hydroxide (Merck), nutrient agar (Merck), and acetic acid glacial (Merck). We use microorganisms (*Escherichia coli*) from our laboratory, including aquadest. Guava seed (*Psidium guajava* L.) leaves from Palembang. FTIR Spectrophotometer (Shimadzu Prestige-21), Scanning Electron Microscopy (JEOL JSM 6510 LA), X-ray diffraction (Shimadzu XRD 6000) and UV-Vis spectroscopy (Genesys 150 Thermo Scientific).

2.2 Ethanolic Extract as Medium in Biosynthesis

This medium was prepared by maceration process and followed the procedure from Fatimah et al. (2016) with slight modification. A dry leaf guava seed (25 g) was soaked in ethanol 70% (v/v, 250 mL) in a maceration bottle (24 h). After 24 h, the filtrate was separated and collected in a clean bottle and stored a room temperature for the further experiment (filtrate I). The residue was macerated again with 250 mL ethanol 70% (v/v) (24 h). the mixture was filtered, and the filtrate was collected and merged with filtrate I. All filtrate was stored at a room temperature.

2.3 Biosynthesis of Metal Oxide Nanoparticles

The procedure of biosynthesis was adopted from Fouda et al. (2020) with slight modification. The ethanolic extract of guava seed leaves (75 mL) in a beaker glass 250 mL was added by the solution of zinc acetate dihydrate (0.2743 g, 25 mL) and the concentration of zinc acetate pentahydrate was 0.0124 M. This beaker glass was heated on a hot plate at 80°C for 60 minutes with continuous stirring. The 0.1 M of sodium hydroxide solution (10 mL) was added to this beaker glass with continuous stirring (pH 10). The mixture was stored for one night until the precipitation appeared. The filtrate and residue (ZnO nanoparticles) were separated, and ZnO nanoparticles were washed with aquadest (15 mL) and absolute ethanol (15 mL). The product of ZnO nanoparticles was dried in the oven (60°C) until dry. The same procedure was used to biosynthesis of CuO and ZnO/CuO nanoparticles as seen in Table 1.

2.4 Synthesis of the Film

The synthesis of film A was adopted from Kalia et al. (2021) with slight modification. Chitosan solution in 250 mL of beaker glass (0.1 g of chitosan powder and10 mL of acetic acid solution 1% v/v) was added 0.1 g of ZnO nanoparticles and shaken by continuously stirring (room temperature, 1 h). A polypropylene petri dish with a diameter of 7.4 cm was filled with the chitosan and ZnO nanoparticle solution and left to dry at room temperature. Figure 1 depicts the synthesis's organizational design. The same procedure was used to prepare the films B, C, D, and E, which are listed in Table 2.

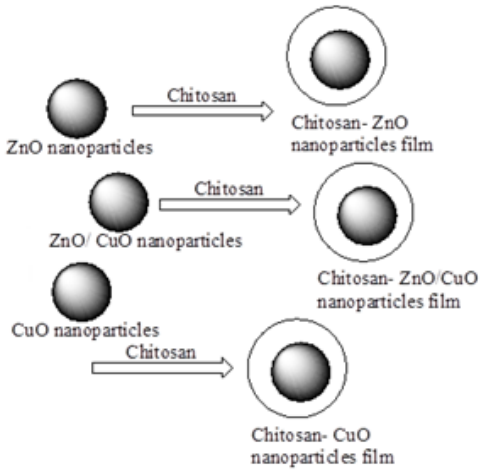

Figure 1. Synthesis Chitosan-metal Oxide Nanoparticles Film

2.5 Characterization

ZnO, CuO and ZnO/CuO nanoparticles were analyzed by UV-Vis Spectrometer to obtain their UV-Vis spectra. The wavelengths ranging from 200 to 550 nm were used to this analysis. ZnO, CuO, ZnO/CuO nanoparticles, and film A-E were characterized by their functional groups with FTIR Spectrophotometer (the region between 4500 and 500 cm^{-1}). X-ray diffraction is used for physical structure analysis of ZnO, CuO, and ZnO/CuO nanoparticles, film A-E, and calculating the crystallite size of ZnO, CuO, and ZnO/CuO nanoparticles. The XRD operational conditions refer to previous literature (Fatoni et al., 2021). The surface morphology of chitosan film, films A, B, and D was characterized by SEM at 15 kV with various magnifications x 3500 (scale bars = 5 μm) and × 10000 (scale bars = 5 μm).

2.6 The Antibacterial Procedure of the Film Chitosan-metal Oxide Nanoparticles

Three petri plates were used in this study. The agar disc diffusion method was used for the identification of chitosan-metal

Table 1. The Materials in the Biosynthesis of Metal Oxide Nanoparticles

The Ethanolic Extract of Guava Seed Leaves (mL)	Zinc Acetate Pentahydrate (g)	Copper Sulphate Pentahydrate (g)	Aquadest (mL)	Sodium Hydroxide Solution (M, mL)	The Name of Product
75	0.2743	-	25	0.1, 10	ZnO Nanoparticles
75	-	0.9363	25	0.1, 13	CuO Nanoparticles
75	0.2743	0.9363	25	0.1, 13	ZnO/CuO Nanoparticles

Table 2. Compares the Use of Nanoparticles of Chitosan, ZnO, CuO, and ZnO/CuO in the Synthesis of All Films

Film	The Comparison between Chitosan and ZnO, CuO and ZnO/CuO Nanoparticles	
	Chitosan (g)	Mass (g) of Metal Oxide Nanoparticles
A	0.1	0.1 (ZnO Nanoparticles)
B	0.1	0.1 (CuO Nanoparticles)
C	0.1	0.1 (ZnO/CuO Nanoparticles)
D	0.1	0.2 (ZnO/CuO Nanoparticles)
E	0.2	0.1 (ZnO/CuO Nanoparticles)

oxide nanoparticles film as an antibacterial agent and the antibacterial procedure was adopted from Fatoni et al. (2022). The procedure from Isnaeni et al. (2020) was used to prepare the inoculum of the bacterial suspension. The film (1 cm × 1 cm) was pasted in the second layer of nutrient agar. The second layer of nutrient agar contained the bacterial suspension. The Petri plate was incubated at 37°C for 24 h. The diameter of the inhibition zone was measured after 24 h.

3. RESULTS AND DISCUSSION

3.1 Biosynthesis Metal Oxide Nanoparticles

The process of biosynthesis of metal oxide nanoparticles was illustrated as seen in Figure 2. The materials were used in the biosynthesis of metal oxide nanoparticles such as ethanolic extract of guava seed leaves, zinc acetate dihydrate, copper sulphate pentahydrate, and sodium hydroxide solution. Ethanolic extract of guava seed leaves are containing active biomolecules: vitamins, tannin, alkaloids, carbohydrates, steroids, glycosides, and flavonoids (Joseph et al., 2016). The biomolecules were activated at pH 10 and this pH, the biomolecules will increase them as a capping and stabilizing agent because of its ability to change the electrical charges of biomolecules (Khalil et al., 2014).

The product of biosynthesis ZnO, CuO and ZnO/CuO nanoparticles as seen in Figure 3. The product of the film as shown in Figure 4.

3.2 UV-Vis Spectroscopy Analysis

The optical properties and electronic structure of metal nanoparticles were analyzed by UV–Vis spectroscopy such as the absorption peaks (Dobrucka et al., 2019). Surface plasmon absorption (SPA) causes absorption peaks (Rajendrachari et al., 2021). The biosynthesis of ZnO, CuO, and ZnO/CuO nanoparticles

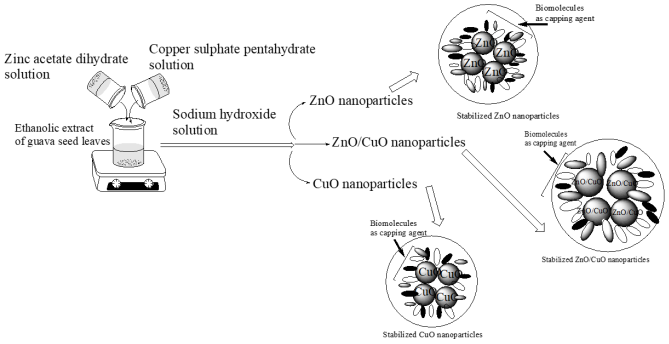

Figure 2. Biosynthesis of Metal Oxide Nanoparticles

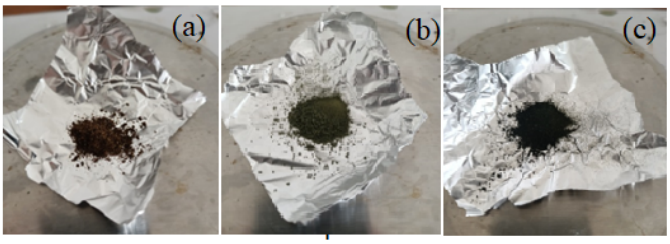

Figure 3. Documentation Picture of ZnO, CuO, and ZnO/CuO Nanoparticles in (a), (b), and (c), Respectively

were analyzed by UV-Vis spectroscopy and shown in Figure 5. In Figure 5, the specific UV absorbance for ZnO, CuO, and ZnO/CuO nanoparticles at 250, 272 and 270 wavelengths respectively. The wavelength at 250 nm for ZnO nanoparticles. This peak is lower than 300 nm and as per the previous literature (Dobrucka and Długaszewska, 2016). The peak at 272 nm for CuO nanoparticles is still below the results of

Table 3. The Inhibition Zone of All Films

Film	The Film of:	The Inhibition Zone (mm)			
		Petri Plate 1	Petri Plate 2	Petri Plate 3	Average ± SD
A	Chitosan-ZnO Nanoparticles	26.36	25.87	25.93	26.03 ± 0.21
B	Chitosan-CuO Nanoparticles	19.48	19.52	17.63	18.87 ± 0.88
C	Chitosan-ZnO/CuO Nanoparticles (Type A)	22.99	20.69	23.53	22.40 ± 1.23
D	Chitosan-ZnO/CuO Nanoparticles (Type B)	26.25	26.98	27.70	26.97 ± 1.53
E	Chitosan-ZnO/CuO Nanoparticles (Type C)	19.38	18.49	19.38	19.08 ± 0.41
F	Chitosan	-	-	-	-

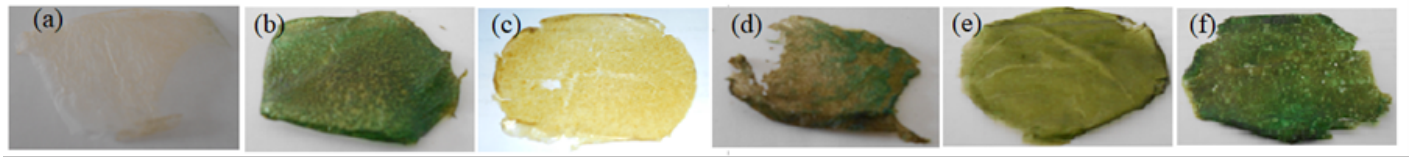

Figure 4. The Photograph of Chitosan Film (a), Chitosan-CuO Nanoparticles Film (b, Film B) and Chitosan-ZnO Nanoparticles Film (c, Film A), Chitosan-ZnO/CuO Nanoparticles Film (d, Film C), Chitosan-ZnO/CuO Nanoparticles Film (e, Film E) and Chitosan-ZnO/CuO Nanoparticles Film (f, Film D)

research by Bhavyasree and Xavier (2020). There is a transition of electrons from the valence band to the conduction band of CuO even with a weak absorption band. The peak for ZnO/CuO nanoparticles at 270 nm is a similar peak to the study of Asamoah et al. (2020). In this peak, the transition from the 2_p of oxygen to the 4_s of Cu^{2+} was observed.

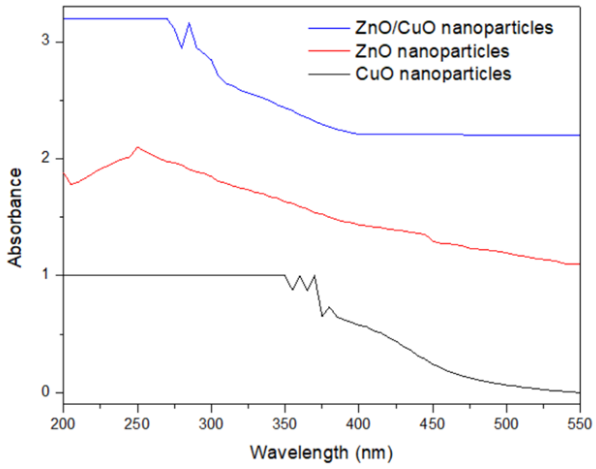

Figure 5. Profile of UV-Vis Spectra ZnO, CuO, and ZnO/CuO Nanoparticles

3.3 Functional Group Analysis

The FTIR spectra of ZnO, CuO and ZnO/CuO nanoparticles as seen in Figure 6.

The interpretation of spectra in Figure 6 shows, the band region at 3423-3448 cm^{-1} can be noted to stretching vibration of O-H and N-H from a secondary metabolite as a bioactive

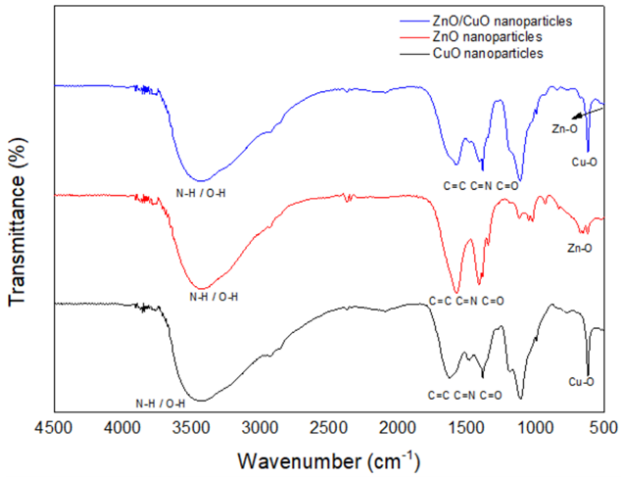

Figure 6. FTIR Spectra of CuO Nanoparticles, ZnO Nanoparticles and ZnO/CuO Nanoparticles

compound (Matinise et al., 2017). The band at 929-1620 cm^{-1} is due to C=C, C=N, and C=O (Matinise et al., 2017). The characteristic of metal oxides has an absorption band below 1000 cm^{-1} because of interatomic vibration (Matinise et al., 2017). The peak at 503 and 619 cm^{-1} is the stretching vibration of the Cu-O (Hemalatha and Makeswari, 2017; Berra et al., 2018; Altikatoglu et al., 2017). The Zn-O (stretching vibration) shows at 468-675 cm^{-1} (Dobrucka and Długaszewska, 2016; Jan et al., 2021; Mydeen et al., 2020) and a stretching vibration of Zn-O/Cu-O observed at 497 and 619 cm^{-1} (Fouda et al., 2020).

The FTIR spectra of chitosan film, film A and B as displayed in Figure 7 and film C, D, and E as seen in Figure 8.

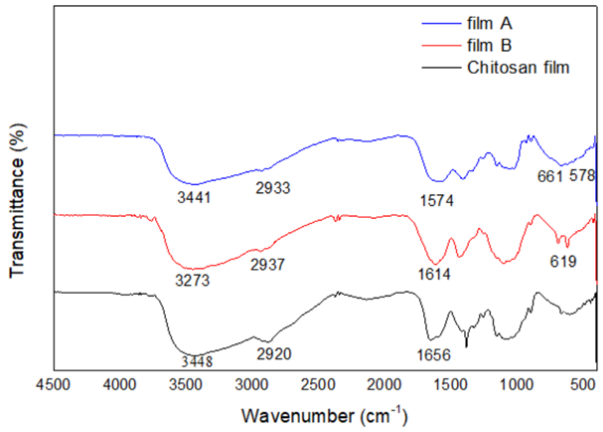

Figure 7. FTIR Spectrum of Chitosan Film, Chitosan-ZnO Nanoparticles Film (Film A) and CuO Nanoparticles Film (Film B)

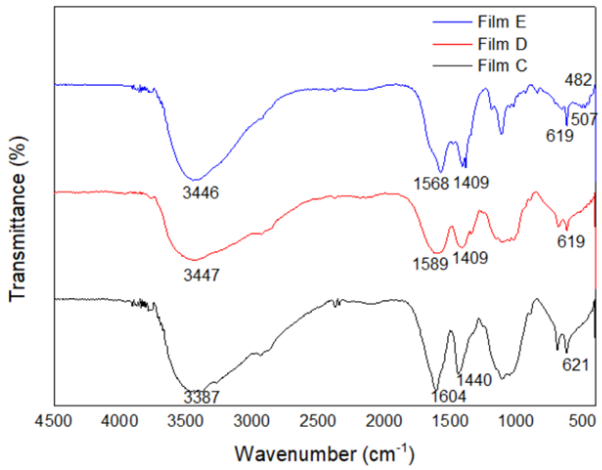

Figure 8. FTIR Spectra of Film C, D and E

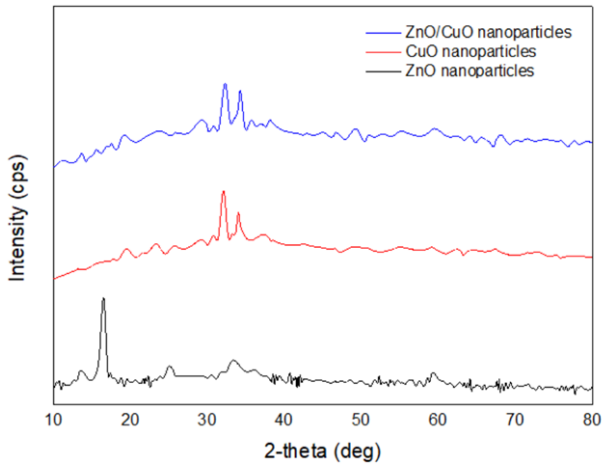

Figure 9. Diffractogram of ZnO Nanoparticles, CuO Nanoparticles and ZnO/CuO Nanoparticles

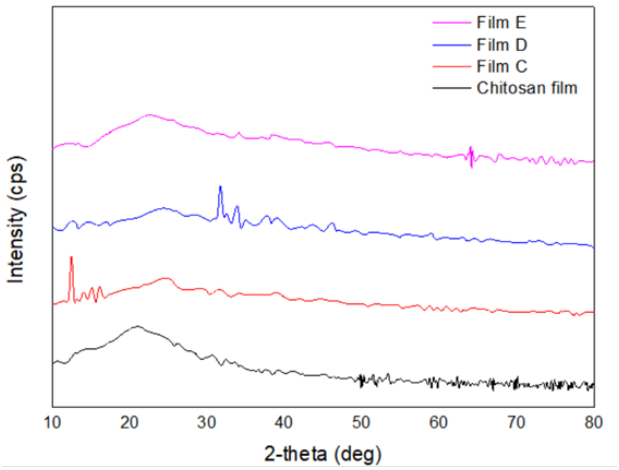

Figure 10. Diffractogram of Chitosan Film, Chitosan-ZnO/CuO Nanoparticles Film (Film C), Chitosan-ZnO/CuO Nanoparticles Film (Film D) and Chitosan-ZnO/CuO Nanoparticles Film (Film E)

Chitosan film (Figure 7) showed bands at 3448 cm^{-1}, 2920 cm^{-1}, 1656 cm^{-1}, and 1595 cm^{-1}, which were investigated to the O-H/N-H stretching, C-H stretching, amide-I, and amide-II groups, respectively (Krishnan et al., 2020). In Figure 7 and 8, the FTIR spectra of film A-E has a characteristic band between 3273 and 3446 cm^{-1} and show the overlap of stretching vibration of –NH and –OH groups. All these bands are lower than a band of stretching vibration of –NH and –OH groups chitosan film (3448 cm^{-1}). The peaks at amide-I of chitosan-ZnO nanoparticles film and chitosan-CuO nanoparticles film shifted to lower wavenumber (1656 to 1574- 1614 cm^{-1}). The decrease in wavenumber shows the interaction of –NH, –OH, and amide-I groups of chitosan with ZnO or CuO through a hydrogen bond (Prokhorov et al., 2020).

3.4 Analysis of Physical Structure

The analysis of physical structure of ZnO, CuO and ZnO/CuO nanoparticles as seen in Figure 9.

The peaks observed at 2θ = 13.95°, 16. 42°, 33.5°, and 59.54° (Figure 9, ZnO nanoparticles). These peaks showed a crystalline form for ZnO nanoparticles (Sharmila et al., 2018; Kalpana et al., 2018). In Figure 9 (CuO nanoparticles), the sharp peak at $2\theta \approx 32.21°$ is a crystalline form for CuO nanoparticles (Murthy et al., 2021). The diffractogram ZnO/CuO nanoparticles has peaks at 2θ values of 32.31°, 34.40° and 60.23°. These peaks are the peaks of CuO nanoparticles (Murthy et al., 2021). The difference between diffractogram of CuO nanoparticles and ZnO/CuO nanoparticles is the presence of ZnO nanoparticles peaks in diffractogram of ZnO/CuO nanoparticles.

The crystallite size of the biosynthesized ZnO, CuO, and ZnO/CuO nanoparticles was calculated by a Debye Scherrer's

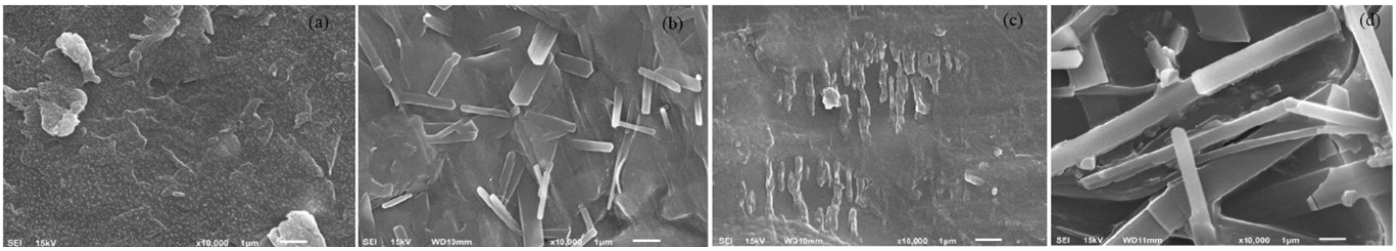

Figure 11. Surface Morphology of Chitosan Film (a), Chitosan-CuO Nanoparticles Film (b), Chitosan-ZnO Nanoparticles Film (c) and Chitosan-ZnO/CuO Nanoparticles Film (d, Film D)

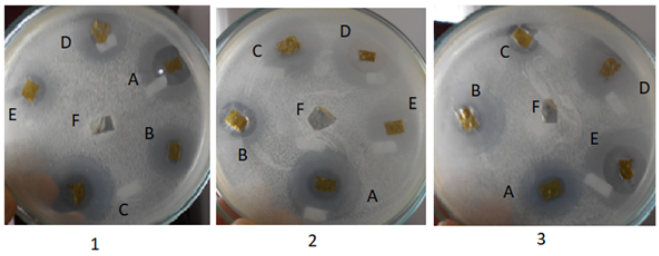

Figure 12. The Antibacterial Study of Film A, B, C, D, E and F (Chitosan Film as Control)

formula (Chinnathambi and Alahmadi, 2021).

$$D = \frac{0.9.\lambda}{\beta.\cos\theta}$$

Where D, λ, β and θ are the crystallite size, the wavelength, the full width at half maximum (FWHM) and Bragg's angle respectively. The crystallite size of the biosynthesized ZnO, CuO, and ZnO/CuO nanoparticles were estimated 13.21, 13.21 and 11.49 nm respectively.

The physical structure of chitosan film, chitosan-ZnO/CuO nanoparticles film, chitosan-ZnO/CuO nanoparticles film, and chitosan-ZnO/CuO nanoparticles film as seen in Figure 10.

The XRD pattern of chitosan film (Figure 10) shows the peak at $2\theta \approx 14.3°$ and 20.6°. These peaks are in hydrate crystalline form (Prokhorov et al., 2020). The peaks that appeared in the chitosan-ZnO/CuO nanoparticles film (film C, Figure 10) have $2\theta \approx 12.44°$, 15.17°, 24.70° and 64.00°. The XRD pattern of film D (Figure 10) shows the peak at $2\theta \approx 24.30°$, 31.59°, 37.58°, and 77.10°. Film E (Figure 10) contained $2\theta \approx 11.00°$, 22.70° and 66°. The peak of 2θ chitosan in films C and E was detected at 12.44° and 11.00° respectively. This peak is lower than the peak of film chitosan and showed an increase in the degree of amorphous form because of the interaction between the N-H and O-H groups in chitosan with ZnO/CuO nanoparticles (Prokhorov et al., 2020). The peak of chitosan in film D was observed at $2\theta = 24.30°$, Sharma et al. (2012) reported that the peak at $2\theta = 24°$ was the amorphous region of the film chitosan. In the film, C, D, and E, the peaks of ZnO/CuO nanoparticles were observed as reported in previous study (Sharmila et al., 2018; Logpriya et al., 2018) and showed that chitosan associated with ZnO and CuO nanoparticles.

3.5 Analysis of Surface Morphology

The scanning electron micrographs for chitosan and modified chitosan as seen in Figure 11.

The SEM image of a chitosan film (Figure 11(a)) showed that it had a nonporous surface and irregular form depending on the degree of acetylation and molecular weight (López-Mata et al., 2013). the addition of ZnO, CuO, and ZnO/CuO nanoparticles in chitosan caused morphological differences at the surfaces of the film (Figure 11(b,c,d)). The interaction of metal oxide nanoparticles can change the chitosan surface (Aljuhani et al., 2021). The surface of chitosan-ZnO/CuO nanoparticles film is different than chitosan-ZnO nanoparticles film or chitosan-CuO nanoparticles film because the amount of Cu^{2+} ion is higher than Zn^{2+} ion.

3.6 Antibacterial Study of All Films

The antibacterial study of all films was investigated using the agar diffusion method. This method is simple, cheap, can be used to test a high number of microorganisms and antimicrobial as sample and the ease to explain the results of the data obtained (Balouiri et al., 2016). The data can be seen in Figure 12. The inhibition zone of all films was calculated and tabulated in Table 3.

Table 3 showed the average zone of inhibition of D > A > C > E > B > F film against *Escherichia coli* bacteria. The presence of ZnO or CuO nanoparticles in the A-E films can increase the antimicrobial properties of the film. The mechanism of the film A-D is the antimicrobial activity as reported by the previous literature. The existence of pores in the outer cell wall of *Escherichia coli* bacteria can accelerate ZnO or CuO nanoparticles go into the pores (El Fawal et al., 2020), ZnO or CuO nanoparticles will release the reactive oxygen species (ROS) and Zn^{2+} or Cu^{2+}. Both of them will attack the negative charge of the bacterial cell wall and its effect, disturbing the synthesis of protein of bacteria (Rahman et al., 2018). Dananjaya et al. (2018) as previous researcher concluded that electrostatic attraction can inhibit the growth of bacteria due to the interaction of the positive surface charges of chitosan-metal oxide nanoparticles and the negative charge of the bacterial cell walls.

4. CONCLUSION

ZnO, CuO, and ZnO/CuO nanoparticles can be biosynthesized successfully and the third of metal oxide nanoparticles were used as material in the synthesis of chitosan-metal oxide nanoparticles film. The FTIR spectrum from metal oxide nanoparticles and all films indicated the functional group and structure of metal oxide nanoparticles. XRD pattern of metal oxide nanoparticles and all films indicated the crystalline of metal oxide nanoparticles and amorphous form respectively. The surface morphology of the D film is clear than the chitosan film. The antibacterial activity of D film is higher than A, B, C, and E.

5. ACKNOWLEDGMENT

We would like to thank STIFI Bhakti Pertiwi for funding this research. Thank you to Laboratorium Fisika Terpadu ITB for the morphology surface analysis.

REFERENCES

Adeyemi, J. O., D. C. Onwudiwe, and A. O. Oyedeji (2022). Biogenic Synthesis of CuO, ZnO, and CuO–ZnO Nanoparticles Using Leaf Extracts of *Dovyalis caffra* and their Biological Properties. *Molecules*, **27**(10); 3206

Al-Dahash, G., W. Mubder Khilkala, and S. N. Abd Alwahid (2018). Preparation and Characterization of ZnO Nanoparticles by Laser Ablation in NaOH Aqueous Solution. *Iranian Journal of Chemistry and Chemical Engineering*, **37**(1); 11–16

Aljuhani, A., S. M. Riyadh, and K. D. Khalil (2021). Chitosan/CuO Nanocomposite Films Mediated Regioselective Synthesis of 1, 3, 4-trisubstituted Pyrazoles under Microwave Irradiation. *Journal of Saudi Chemical Society*, **25**(8); 101276

Altikatoglu, M., A. Attar, F. Erci, C. M. Cristache, I. Isildak, et al. (2017). Green Synthesis of Copper Oxide Nanoparticles Using *Ocimum basilicum* Extract and their Antibacterial Activity. *Fresenius Environmental Bulletin*, **25**(12); 7832–7837

Alzahrani, E. (2018). Chitosan Membrane Embedded with ZnO/CuO Nanocomposites for the Photodegradation of Fast Green Dye under Artificial and Solar Irradiation. *Analytical Chemistry Insights*, **13**; 1177390118763361

Asamoah, R., A. Yaya, B. Mensah, P. Nbalayim, V. Apalangya, Y. Bensah, L. Damoah, B. Agyei-Tuffour, D. Dodoo-Arhin, and E. Annan (2020). Synthesis and Characterization of Zinc and Copper Oxide Nanoparticles and their Antibacteria Activity. *Results in Materials*, **7**; 100099

Balouiri, M., M. Sadiki, and S. K. Ibnsouda (2016). Methods for in Vitro Evaluating Antimicrobial Activity: A Review. *Journal of Pharmaceutical Analysis*, **6**(2); 71–79

Berra, D., S. Laouini, B. Benhaoua, M. Ouahrani, D. Berrani, and A. Rahal (2018). Green Synthesis of Copper Oxide Nanoparticles by *Pheonix dactylifera* L Leaves Extract. *Digest Journal of Nanomaterials and Biostructures*, **13**(4); 1231–1238

Bhavyasree, P. and T. Xavier (2020). Green Synthesis of Copper Oxide/Carbon Nanocomposites Using the Leaf Extract of *Adhatoda vasica* Nees, their Characterization and Antimicrobial Activity. *Heliyon*, **6**(2); e03323

Bloch, K., K. Pardesi, C. Satriano, and S. Ghosh (2021). Bacteriogenic Platinum Nanoparticles for Application in Nanomedicine. *Frontiers in Chemistry*, **9**; 624344

Cao, Y., H. A. Dhahad, M. El-Shorbagy, H. Q. Alijani, M. Zakeri, A. Heydari, E. Bahonar, M. Slouf, M. Khatami, M. Naderifar, et al. (2021). Green Synthesis of Bimetallic ZnO–CuO Nanoparticles and their Cytotoxicity Properties. *Scientific Reports*, **11**(1); 23479

Chinnathambi, A. and T. A. Alahmadi (2021). Zinc Nanoparticles Green-synthesized by Alhagi maurorum Leaf Aqueous Extract: Chemical Characterization and Cytotoxicity, Antioxidant, and Anti-osteosarcoma Effects. *Arabian Journal of Chemistry*, **14**(4); 103083

Dananjaya, S., R. S. Kumar, M. Yang, C. Nikapitiya, J. Lee, and M. De Zoysa (2018). Synthesis, Characterization of ZnO-chitosan Nanocomposites and Evaluation of its Antifungal Activity Against Pathogenic *Candida albicans*. *International Journal of Biological Macromolecules*, **108**; 1281–1288

Das, S. and V. C. Srivastava (2017). Synthesis and Characterization of ZnO/CuO Nanocomposite by Electrochemical Method. *Materials Science in Semiconductor Processing*, **57**; 173–177

Dobrucka, R. and J. Długaszewska (2016). Biosynthesis and Antibacterial Activity of ZnO Nanoparticles Using *Trifolium pratense* Flower Extract. *Saudi Journal of Biological Sciences*, **23**(4); 517–523

Dobrucka, R., M. Kaczmarek, M. Łagiedo, A. Kielan, and J. Dlugaszewska (2019). Evaluation of Biologically Synthesized Au-CuO and CuO-ZnO Nanoparticles Against Glioma Cells and Microorganisms. *Saudi Pharmaceutical Journal*, **27**(3); 373–383

El Fawal, G., H. Hong, X. Song, J. Wu, M. Sun, C. He, X. Mo, Y. Jiang, and H. Wang (2020). Fabrication of Antimicrobial Films Based on Hydroxyethylcellulose and ZnO for Food Packaging Application. *Food Packaging and Shelf Life*, **23**; 100462

Estevam, L. d. S., H. S. Debone, C. M. P. Yoshida, and C. Da Silva (2012). Adsorption of Bovine Serum and Bovine Haemoglobin onto Chitosan Film. *Adsorption Science and Technology*, **30**(8-9); 785–792

Fatimah, I., R. Y. Pradita, and A. Nurfalinda (2016). Plant Extract Mediated of ZnO Nanoparticles by Using Ethanol Extract of *Mimosa pudica* Leaves and Coffee Powder. *Procedia Engineering*, **148**; 43–48

Fatoni, A., M. A. Afrizal, A. A. Rasyad, and N. i Hidayat (2021). ZnO Nanoparticles and Its Interaction With Chitosan: Profile Spectra and Their Activity Against Bacterial. *JKPK (Jurnal Kimia dan Pendidikan Kimia)*, **6**(2); 216–227

Fatoni, A., H. S. Yessica, M. Almi, A. Rendowaty, L. Sirumapea, N. Hidayati, et al. (2022). The Film of Chitosan-ZnO Nanoparticles-CTAB: Synthesis, Characterization and In

Vitro Study. *Science and Technology Indonesia*, **7**(1); 58–66
Foster, L. J. R. and J. Butt (2011). Chitosan Films are NOT Antimicrobial. *Biotechnology Letters*, **33**; 417–421
Fouda, A., S. S. Salem, A. R. Wassel, M. F. Hamza, and T. I. Shaheen (2020). Optimization of Green Biosynthesized Visible Light Active CuO/ZnO Nano-photocatalysts for the Degradation of Organic Methylene Blue Dye. *Heliyon*, **6**(9); e04896
Gondal, M., T. F. Qahtan, M. A. Dastageer, Y. Maganda, D. H. Anjum, et al. (2013). Synthesis of Cu/Cu2O Nanoparticles by Laser Ablation in Deionized Water and their Annealing Transformation into CuO Nanoparticles. *Journal of Nanoscience and Nanotechnology*, **13**(8); 5759–5766
Goyal, C., D. Goyal, N. S. Ramgir, M. Navaneethan, Y. Hayakawa, C. Muthamizhchelvan, H. Ikeda, and S. Ponnusamy (2021). Surface Modification of ZnO Nanowires with CuO: A Tool to Realize Highly-sensitive H_2S Sensor. *Physics of the Solid State*, **63**; 460–467
Hemalatha, S. and M. Makeswari (2017). Green Synthesis, Characterization and Antibacterial Studies of CuO Nanoparticles from *Eichhornia crassipes*. *Rasayan Journal of Chemistry*, **10**(3); 838–843
Isnaeni, I., E. Hendradi, and N. Z. Zettira (2020). Inhibitory Effect of Roselle Aqueous Extracts-HPMC 6000 Gel on the Growth of *Staphylococcus aureus* ATCC 25923. *Turkish Journal of Pharmaceutical Sciences*, **17**(2); 190–196
Jan, F. A., R. Ullah, N. Ullah, M. Usman, et al. (2021). Exploring the Environmental and Potential Therapeutic Applications of *Myrtus communis* L. Assisted Synthesized Zinc Oxide (ZnO) and Iron Doped Zinc Oxide (Fe-ZnO) Nanoparticles. *Journal of Saudi Chemical Society*, **25**(7); 101278
Jayaramudu, T., K. Varaprasad, R. D. Pyarasani, K. K. Reddy, K. D. Kumar, A. Akbari-Fakhrabadi, R. Mangalaraja, and J. Amalraj (2019). Chitosan Capped Copper Oxide/copper Nanoparticles Encapsulated Microbial Resistant Nanocomposite Films. *International Journal of Biological Macromolecules*, **128**; 499–508
Joseph, L., M. George, G. Singh, and P. Mathews (2016). Phytochemical Investigation on Various Parts of *Psidium guajava*. *Annals of Plant Sciences*, **5**(2); 1265–1268
Kalia, A., M. Kaur, A. Shami, S. K. Jawandha, M. A. Alghuthaymi, A. Thakur, and K. A. Abd-Elsalam (2021). Nettle-leaf Extract Derived ZnO/CuO Nanoparticle-biopolymer-based Antioxidant and Antimicrobial Nanocomposite Packaging Films and their Impact on Extending the Post-harvest Shelf Life of Guava Fruit. *Biomolecules*, **11**(2); 224
Kalpana, V., B. A. S. Kataru, N. Sravani, T. Vigneshwari, A. Panneerselvam, and V. D. Rajeswari (2018). Biosynthesis of Zinc Oxide Nanoparticles Using Culture Filtrates of *Aspergillus niger*: Antimicrobial Textiles and Dye Degradation Studies. *OpenNano*, **3**; 48–55
Khalil, M. M., E. H. Ismail, K. Z. El-Baghdady, and D. Mohamed (2014). Green Synthesis of Silver Nanoparticles Using Olive Leaf Extract and its Antibacterial Activity. *Arabian Journal of Chemistry*, **7**(6); 1131–1139
Krishnan, R. A., O. Mhatre, J. Sheth, S. Prabhu, R. Jain, and P. Dandekar (2020). Synthesis of Zinc Oxide Nanostructures Using Orange Peel Oil for Fabricating Chitosan-zinc Oxide Composite Films and their Antibacterial Activity. *Journal of Polymer Research*, **27**; 1–13
Logpriya, S., V. Bhuvaneshwari, D. Vaidehi, R. SenthilKumar, R. Nithya Malar, B. Pavithra Sheetal, R. Amsaveni, and M. Kalaiselvi (2018). Preparation and Characterization of Ascorbic Acid-mediated chitosan–copper Oxide Nanocomposite for Anti-microbial, Sporicidal and Biofilm-inhibitory Activity. *Journal of Nanostructure in Chemistry*, **8**; 301–309
López-Mata, M. A., S. Ruiz-Cruz, N. P. Silva-Beltrán, J. D. J. Ornelas-Paz, P. B. Zamudio-Flores, and S. E. Burruel-Ibarra (2013). Physicochemical, Antimicrobial and Antioxidant Properties of Chitosan Films Incorporated with Carvacrol. *Molecules*, **18**(11); 13735–13753
Matinise, N., X. Fuku, K. Kaviyarasu, N. Mayedwa, and M. Maaza (2017). ZnO Nanoparticles via *Moringa oleifera* Green Synthesis: Physical Properties and Mechanism of Formation. *Applied Surface Science*, **406**; 339–347
Mohamed, E. A. (2020). Green Synthesis of Copper and Copper Oxide Nanoparticles Using the Extract of Seedless Dates. *Heliyon*, **6**(1); 03123
Murthy, H. A., T. D. Zeleke, K. Tan, S. Ghotekar, M. W. Alam, R. Balachandran, K.-Y. Chan, P. Sanaulla, M. A. Kumar, and C. Ravikumar (2021). Enhanced Multifunctionality of CuO Nanoparticles Synthesized Using Aqueous Leaf Extract of *Vernonia amygdalina* plant. *Results in Chemistry*, **3**; 100141
Mydeen, S. S., R. R. Kumar, M. Kottaisamy, and V. Vasantha (2020). Biosynthesis of ZnO Nanoparticles through Extract from *Prosopis juliflora* Plant Leaf: Antibacterial Activities and a New Approach by Rust-induced Photocatalysis. *Journal of Saudi Chemical Society*, **24**(5); 393–406
Naveed Ul Haq, A., A. Nadhman, I. Ullah, G. Mustafa, M. Yasinzai, I. Khan, et al. (2017). Synthesis Approaches of Zinc Oxide Nanoparticles: the Dilemma of Ecotoxicity. *Journal of Nanomaterials*, **2017**; 1–14
Pantidos, N. and L. E. Horsfall (2014). Biological Synthesis of Metallic Nanoparticles by Bacteria, Fungi and Plants. *Journal of Nanomedicine and Nanotechnology*, **5**(5); 233
Prokhorov, E., G. Luna-Bárcenas, J. M. Yáñez Limón, A. Gómez Sánchez, and Y. Kovalenko (2020). Chitosan-ZnO Nanocomposites Assessed by Dielectric, Mechanical, and Piezoelectric Properties. *Polymers*, **12**(9); 1991
Rahman, P. M., V. A. Mujeeb, K. Muraleedharan, and S. K. Thomas (2018). Chitosan/nano ZnO Composite Films: Enhanced Mechanical, Antimicrobial and Dielectric Properties. *Arabian Journal of Chemistry*, **11**(1); 120–127
Rajendrachari, S., P. Taslimi, A. C. Karaoglanli, O. Uzun, E. Alp, and G. K. Jayaprakash (2021). Photocatalytic Degradation of Rhodamine B (RhB) Dye in Waste Water and Enzymatic Inhibition Study Using Cauliflower Shaped ZnO Nanoparticles Synthesized by a Novel One-pot Green Synthesis Method. *Arabian Journal of Chemistry*, **14**(6); 103180

Saravanakkumar, D., S. Sivaranjani, K. Kaviyarasu, A. Ayeshamariam, B. Ravikumar, S. Pandiarajan, C. Veeralakshmi, M. Jayachandran, and M. Maaza (2018). Synthesis and Characterization of ZnO–CuO Nanocomposites Powder by Modified Perfume Spray Pyrolysis Method and its Antimicrobial Investigation. *Journal of Semiconductors*, **39**(3); 033001

Sharma, S., P. Sanpui, A. Chattopadhyay, and S. S. Ghosh (2012). Fabrication of Antibacterial Silver Nanoparticle-sodium Alginate-chitosan Composite Films. *RSC Advances*, **2**(13); 5837–5843

Sharmila, G., C. Muthukumaran, K. Sandiya, S. Santhiya, R. S. Pradeep, N. M. Kumar, N. Suriyanarayanan, and M. Thirumarimurugan (2018). Biosynthesis, Characterization, and Antibacterial Activity of Zinc Oxide Nanoparticles Derived from *Bauhinia tomentosa* Leaf Extract. *Journal of Nanostructure in Chemistry*, **8**; 293–299

Shinde, R. S., S. D. Khairnar, M. R. Patil, V. A. Adole, P. B. Koli, V. V. Deshmane, D. K. Halwar, R. A. Shinde, T. B. Pawar, and B. S. Jagdale (2022). Synthesis and Characterization of ZnO/CuO Nanocomposites as an Effective Photocatalyst and Gas Sensor for Environmental Remediation. *Journal of Inorganic and Organometallic Polymers and Materials*; 1–22

Solanki, P. R., A. Kaushik, V. V. Agrawal, and B. D. Malhotra (2011). Nanostructured Metal Oxide-based Biosensors. *NPG Asia Materials*, **3**(1); 17–24

Zhang, D., X.-l. Ma, Y. Gu, H. Huang, and G.-w. Zhang (2020). Green Synthesis of Metallic Nanoparticles and their Potential Applications to Treat Cancer. *Frontiers in Chemistry*, **8**; 799

